Diffusion of Exchangeable Water in Cortical Bone Studied by Nuclear Magnetic Resonance

Maria A. Fernández-Seara,* Suzanne L. Wehrli,† and Felix W. Wehrli*
*Laboratory for Structural NMR Imaging, Department of Radiology, University of Pennsylvania Medical Center, Philadelphia, Pennsylvania; and †NMR Core Facility, Children Hospital, Philadelphia, Pennsylvania

ABSTRACT The rate-limiting step in the delivery of nutrients to osteocytes and the removal of cellular waste products is likely diffusion. The transport of osteoid water across the mineralized matrix of bone was studied by proton nuclear magnetic resonance spectroscopy and imaging by measuring the diffusion fluxes of tissue water in cortical bone specimens from the midshaft of rabbit tibiae immersed in deuterium oxide. From the diffusion coefficient ($D_a = (7.8 \pm 1.5) \times 10^{-7}$ cm^2/s) measured at 40°C (close to physiological temperature), it can be inferred that diffusive transport of small molecules from the bone vascular system to the osteocytes occurs within minutes. The activation energy for water diffusion, calculated from D_a measured at four different temperatures, suggests that the interactions between water molecules and matrix pores present significant energy barriers to diffusion. The spatially resolved profile of D_a perpendicular to the cortical surface of the tibia, obtained using a finite difference model, indicates that diffusion rates are higher close to the endosteal and periosteal surfaces, decreasing toward the center of the cortex. Finally, the data reveal a water component (~30%) diffusing four orders of magnitude more slowly, which is ascribed to water tightly bound to the organic matrix and mineral phase.

INTRODUCTION

Mineralized bone tissue contains a significant water fraction, which for cancellous bone can amount up to 20% of its wet weight (Mueller et al., 1966). Skeletally mature cortical bone, however is a denser material in which the fraction of water is reduced to ~10% (Robinson and Elliot, 1957). The fractional water content in bone remains similar across species for the same type of bone, however within a single species it varies with age, sex, and disease state (Timmins and Wall, 1977). Variations in the amount of water are related to changes in the degree of mineralization of the calcified bone matrix. During mineralization of the osteoid, water is gradually replaced by calcium apatatite, which fills the volume previously occupied by water, because the osteoid volume does not change during calcification (Robinson and Elliot, 1957; Neuman and Neuman, 1958). Thus, in some pathological conditions, such as in osteomalacia, an abnormal decrease in mineral content occurs concurrently with an increase in water content (Mueller et al., 1966).

Water in bone may be found associated with the mineral phase, bound to the organic phase (collagen and cement substance), or free (bulk water). Bulk water fills the pores of the calcified matrix, which form a network of interconnecting channels (the lacunocanalicular system), which communicate the Haversian canals (the bone vascular system) with the osteocytes, embedded in the mineralized matrix. This communication network serves for transport of nutrients, waste products, and signaling molecules from the vascular system to the osteocytes and vice versa. The water channels are also the transport pathways for calcium and phosphate ions flowing in and out of bone tissue, which acts as a mineral reservoir for the rest of the organism.

In recent years, significant efforts have been expended to elucidate the nature of the fluid transport mechanisms through the bone matrix and to determine the extent of diffusive transport as the rate-limiting step in the supply of nutrients to the osteocytes (Tate and Knothe, 2000; Tate et al., 1998; Dillaman et al., 1991). Up to date, most reported work has been limited to qualitative descriptions of transport pathways, obtained empirically by means of molecular tracers (Tate et al., 1998; Ayasaka et al., 1992; Sasaki et al., 1985). Quantitative information thus is scarce (Neuman and Neuman, 1981; Edelman et al., 1954). Diffusion measurements in bone are complicated by the heterogeneity of the tissue microstructure. Nonetheless, quantitative diffusion data can provide estimates of transport times and fluxes of matter through the tissue, as well as information on matrix porosity and insight on the function and location of the water contained in the matrix pores.

The purpose of this study was to investigate the dynamics of the osteoid water exchange and to measure the apparent diffusion coefficient of water in cortical bone specimens from the shaft of rabbit tibiae by means of proton nuclear magnetic resonance (NMR) spectroscopy and imaging. The experimental method was based on monitoring the time dependence of the exchange of tissue water while the bone was immersed in deuterium oxide (D_2O), by measuring the net flux of H_2O into the D_2O pool. The decrease in intraosseous H_2O concentration and the changes in its spatial distribution along the direction perpendicular to the cortical surface were observed during the exchange process by proton imaging. The time-varying water concentration pat-

Received for publication 1 August 2001 and in final form 3 October 2001.
Address reprint requests to Dr. Felix W. Wehrli, Laboratory for Structural NMR Imaging, Department of Radiology, 1 Silverstein, University of Pennsylvania Medical Center, 3400 Spruce Street, Philadelphia, PA 19104. Tel.: 215-662-7951; Fax: 215-349-5925; E-mail: wehrli@oasis.rad.upenn.edu.

0006-3495/02/01/522/08 $2.00

TABLE 1 Average dimensions and weight of the cortical bone specimens analyzed

Specimen	Length (mm)	Width (mm)	Thickness (mm)	Weight (mg)
1	9.1	4	0.8	47.6
2	9.6	4	0.8	49.2
3	7.5	3.8	0.7	39.7
4	8.1	3	0.75	34.5

terns were then used to compute a spatially resolved diffusion coefficient profile by means of a finite difference approximation of the diffusion equation.

MATERIALS AND METHODS

Four cortical bone specimens were harvested from sections of the diaphysis of two excised tibiae from 5- to 6-month-old New Zealand White rabbits (skeletally mature) after removal of the marrow (by immersing the diaphysis sections in 2.6% sodium hypochlorite in an ultrasonic bath for 30 min and rinsing with a water jet). The specimens were cut into a rectangular plate-like shape with the longest dimension (length) parallel to the tibial axis, the second dimension (width) along the surface of the tibia, while the third dimension matched the thickness of the tibial cortex. The dimensions of the specimens were measured using a digital caliper (Table 1). The specimens were allowed to attain air-stable weight, which is defined as "wet weight."

Diffusion of exchangeable water at 25°C

The diffusion of exchangeable water through the cortical bone matrix was observed using proton NMR spectroscopy. The plate-like samples were placed in a 5-mm NMR tube containing 0.6 ml of deuterium oxide (D_2O, 99.9% isotopic purity, Sigma Chemical Co., St. Louis, MO). The proton-deuterium exchange kinetics at 25°C was followed by proton NMR of the solution, over a period of 6 h (during which an equilibrium state was reached). Spectra were acquired on a vertical-bore superconducting spectrometer system, operating at 9.4T (DMX-400, Bruker Instruments, Karlsruhe, Germany). A capillary containing chloroform ($CHCl_3$) was used as internal reference, to monitor the stability of the spectrometer. Spectra were collected by pulsing continuously with a 20° flip angle radio-frequency (RF) pulse and 16,384 data points were sampled in 3.4 s, corresponding to a spectral width of 2.42 kHz. Four signal averages were collected per free induction decay during a total acquisition time of 13.6 s. The temporal resolution was adjusted to the rate of change of the signal found in preliminary experiments (first hour, 2 min; second hour, 5 min; remainder of experiment, 10 min).

The water peak spectral integral is proportional to the amount of water having diffused from the bone into the solution. Because the cortical bone samples were shaped as thin plates (Table 1), the proton-deuterium exchange was dominated by diffusion along the thickness of the sample. If the bone matrix is considered as an homogeneous medium and the diffusion coefficient is taken to be constant, there exists an analytical solution (Crank, 1957):

$$I(t) = I(\infty)\left[1 - \frac{8}{\pi^2}\sum_{n=0}^{\infty}\frac{1}{(2n+1)^2}\,e^{-\frac{D_a(2n+1)^2\pi^2 t}{d^2}}\right] \quad (1)$$

in which $I(\infty)$ is the integrated signal intensity at equilibrium, D_a is the apparent diffusion coefficient of water through the bone matrix, d is the specimen thickness, and t is the exchange time. For small values of t, Eq. 1 can be approximated by:

$$I(t) = I(\infty)\,\frac{4}{\pi^{1/2}}\left(\frac{D_a t}{d^2}\right)^{1/2} \quad (2)$$

The water peak integral (for small values of time), plotted versus the square root of exchange time was fitted to a straight line and the slope of the regression line used to compute D_a. $I(\infty)$ was estimated from the average of the last six experimental data points after subtracting the integral corresponding to the initial amount of water in the deuterium oxide (due to incomplete deuteration).

Measurement of water content

The amount of exchangeable water was measured using $I(\infty)$ as input in a calibration curve, which was obtained with five solutions of water in 0.6 ml D_2O with water content ranging from 1 to 15 μl, covering the range of water concentration expected in the cortical bone specimens. Proton spectra were acquired with the same acquisition parameters used for the exchange experiments. The experimental data points were least-square fit to a straight line.

The amount of water of the bone specimens was measured using a gravimetric method. The specimens were dried in an oven at 100°C for 48 h, weighed after drying (dry weight) and the water content calculated as the difference between wet and dry weights.

Energy of activation

The temperature dependence of water diffusion in the cortical bone matrix was studied in two of the samples (1 and 3) by measuring the diffusion coefficient at four different temperatures: 25, 40, 55, and 70°C. The diffusion coefficient increases with temperature asymptotically (Stein, 1962):

$$D_a(T) = D_0 e^{-\frac{E_a}{RT}} \quad (3)$$

in which D_0 is a constant independent of temperature, E_a is the activation energy for diffusion, and R is Boltzman's constant. Arrhenius plots were then constructed, and the energy of activation computed from the slope of the regression line obtained by fitting the experimental data points.

Projection imaging of water diffusion

In the experiments described above, diffusion of water across the bone matrix was observed indirectly by measuring the net flux of H_2O from bone into the D_2O solution. It is possible, however, to directly detect the decrease in concentration of the matrix H_2O as it is replaced by (unobservable) D_2O, using proton NMR imaging techniques. The relaxation properties of the NMR signal of bone water protons allow the acquisition of one-dimensional projection images of bone water with sufficient temporal resolution to monitor the H_2O/D_2O exchange process.

One-dimensional projections were obtained by sampling the NMR-free induction decay signal in the presence of a magnetic field gradient, G, applied along the thickness of the specimen. The bone specimen was kept in a predetermined position in the 5-mm tube by using a support specially designed for the experiment. The pulse sequence was programmed using Paravision 2.1 (Bruker Instruments, Karlsruhe, Germany) and the data acquired with the spectrometer previously described.

The free-induction signal decays very rapidly due to the short transverse relaxation time of bone water protons (T_2 = 250 μs (Borthakur et al., 1998)), therefore the receiver dead time must be minimized to reduce signal loss. This was achieved by means of a short rectangular RF pulse

used to excite the spins in the presence of the gradient, which was switched on immediately before the pulse was applied. In this manner the delay between the end of the pulse and the start of data acquisition was reduced to 6 μs.

The imaging parameters were as follows: pulse length, 6 μs (60° flip angle); number of complex points, 256; spectral width, 250 kHz; 64 averages. A gradient of 90 G/cm was used to provide a nominal spatial resolution of 25 μm, which was adequate to resolve the water profile. A repetition time of 120 ms was used to saturate the signal from the water protons in the deuterium oxide solution, which have a longitudinal relaxation time T_1 on the order of 10 s, whereas maximizing the signal from the bone water protons, of shorter T_1 ($T_1 \approx 300$ ms, (Borthakur et al., 1998)). The total scan time was 8 s, thus providing sufficient temporal resolution to map the exchange process. Profiles were acquired every 30 s during the initial 30 min of the experiment, after which the time interval was adjusted to the decay rate of the water concentration (following hour, 10 min; subsequent 15 h, 30 min; remainder of experiment, 60 min; total experiment time, 22 h).

Spatial distribution of the D_a

The spatial distribution of D_a along the tibial cortex was resolved using the water concentration profiles of specimen 2 (Fig. 4) acquired during the initial 10 min of the proton-deuterium exchange with a temporal resolution (δt) of 30 s. This was accomplished using a finite difference approximation of the diffusion equation, which for a spatially variant diffusion coefficient $D(x)$ becomes (Crank, 1957):

$$\frac{\partial c}{\partial t} = \frac{\partial D(x)}{\partial x}\frac{\partial c}{\partial x} + D(x)\frac{\partial^2 c}{\partial x^2} \tag{4}$$

in which c, the water concentration, is proportional to the intensity of the profile at location x.

This equation was discretized using the Crank-Nicholson finite difference scheme, which is second-order accurate in time and space. To apply this method, the tibia cortex was divided into a grid of equally spaced points (where the spacing between the points corresponded to the spatial resolution of the profiles, δx), and the following difference approximations were made to time and spatial derivatives:

$$\left(\frac{\partial c}{\partial t}\right)_m^n = \frac{c_m^{n+1} - c_m^n}{\delta t} \tag{5}$$

$$\left(\frac{\partial c}{\partial x}\right)_m^n = \frac{c_m^n - c_{m-1}^n}{\delta x} \tag{6}$$

$$\left(\frac{\partial D}{\partial x}\right)_m = \frac{D_m - D_{m-1}}{\delta x} \tag{7}$$

$$\left(\frac{\partial^2 c}{\partial x^2}\right)_m^n = \frac{1}{2\delta x^2}\left[(c_{m+1}^{n+1} - 2c_m^{n+1} + c_{m-1}^{n+1}) + (c_{m+1}^n - 2c_m^n + c_{m-1}^n)\right] \tag{8}$$

in which c_m^n represents the water concentration at the grid point at position $x_m = x_o + m\,\delta x$, x_o being the location of the center of the tibial cortex, and acquisition time $t_n = t_o + n\,\delta t$, t_o being the starting time of the experiment.

Substituting these expressions in Eq. 4, a linear equation can be written for every node m at every time step n, where the independent variables are the values of D at the grid points. Because the concentration profiles are approximately symmetric with respect to the center of the cortex, the problem can be simplified by working with one-half of the cortex thickness and imposing a boundary condition of no-flux at the center. The values of D at the grid points were obtained by solving the over-determined linear system, by singular value decomposition of the system matrix, using a routine provided by IDL software (Research Systems, Inc., Boulder, CO).

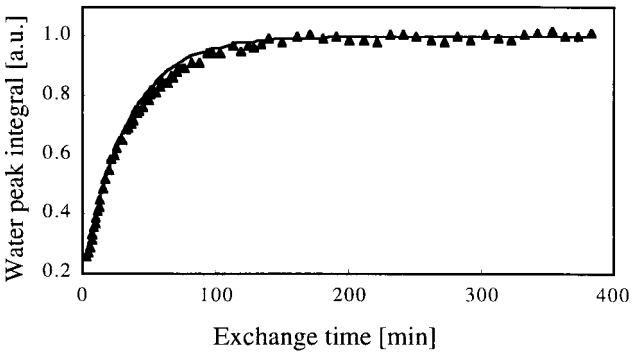

(a)

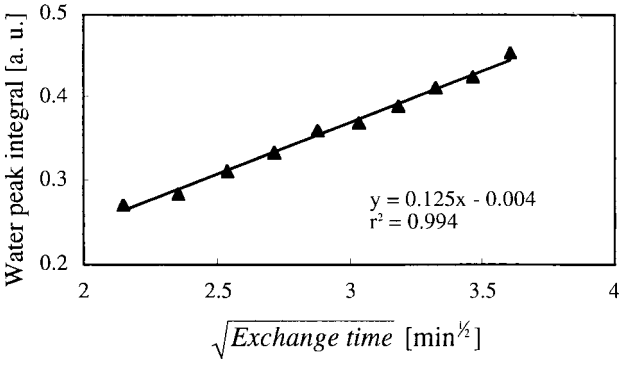

(b)

FIGURE 1 Evolution of the water proton NMR signal for a specimen of cortical bone suspended in D_2O at 25°C. (*a*) Experimental (▲) and simulated (—) exchange kinetics. (*b*) Linear regression line obtained by fitting the ten initial experimental data points. The slope was used to compute D_a from Eq. 2.

RESULTS

Diffusion of exchangeable water at 25°C

Figure 1 *a* shows a typical plot of the integrated water proton spectral peak versus exchange time, obtained at 25°C. A qualitatively similar behavior for proton-deuterium exchange in cortical bone was reported previously in a conference abstract (Borthakur et al., 1998), but no quantitative information was derived in that preliminary work. The regression line determined by fitting the first 10 experimental data points as a function of the square root of the exchange time is depicted in Fig. 1 *b*. We found in simu-

TABLE 2 Water diffusion coefficient (D_a) and exchangeable water in cortical bone from rabbit tibia

Specimen	$D_a \times 10^7$* (cm^2/s)	NMR water (mg)	Water by drying (mg)
1	3.35 ± 0.10	6.04	5.4
2	2.87 ± 0.13	6.03	5.3
3	3.30 ± 0.23	3.03	4.0
4	4.70 ± 0.30	3.39	3.3

*±Standard deviation of regression line slope.

lations that the linear approximation for small values of time (Eq. 2) is reasonable for values of the water peak integral up to 0.5 of the integral at equilibrium. The predicted behavior was corroborated by the experimental data, because r^2 for the linear fit was greater than 0.99 in all the experiments. The D_a values, calculated from the slope of the regression lines (shown in Table 2), were used in simulations to compute a theoretical exchange curve from Eq. 1. Simulated and experimental data are in very good agreement (Fig. 1 *a*). The average value for D_a in cortical bone ((3.56 ± 0.78) × 10^{-7} cm^2/s) at 25°C is smaller than the water diffusion coefficient measured in intertubular dentine ($D_{dentine}$ = (1.74 ± 0.43) × 10^{-6} cm^2/s (van der Graaf and ten Bosch, 1990)), but two orders of magnitude larger than the water diffusion coefficient measured in enamel (D_{enamel} = 3.5 × 10^{-9} to 17 × 10^{-9} cm^2/s (Burke and Moreno, 1975)).

Fig. 2 shows the calibration curve used to determine the amount of exchangeable water of the specimens based on the integrated proton signal intensity at equilibrium. The NMR-derived water content (Table 2) is very close to the one measured using the gravimetric method, thus demonstrating that all or almost all of the water displaced by drying at 100°C is exchangeable.

Energy of activation

As temperature increases diffusion is accelerated, as indicated by the experimental diffusion curves (Fig. 3 *a*). Arrhenius plots obtained for two specimens show excellent linearity (r^2 = 0.997, 0.966 respectively, Fig. 3 *b*). The calculated values for the activation energy (26.8 and 26.6 kJ/mol) are close to E_a for water diffusion in intertubular dentine (E_a = 29.5 kJ/mol, (van der Graaf and ten Bosch, 1991)) and of the order of E_a for water diffusion in enamel (E_a = 21.7 to 61 kJ/mol (Burke and Moreno, 1975)).

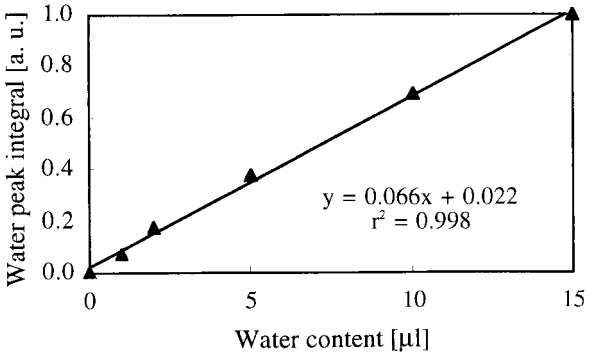

FIGURE 2 Calibration curve for MR-based measurements of exchangeable water. The curve was obtained by adding increasing amounts of water to 0.6 ml D_2O (from 0 to 15 μl), covering the range of water content expected in cortical bone. Integral values were normalized to maximal integral.

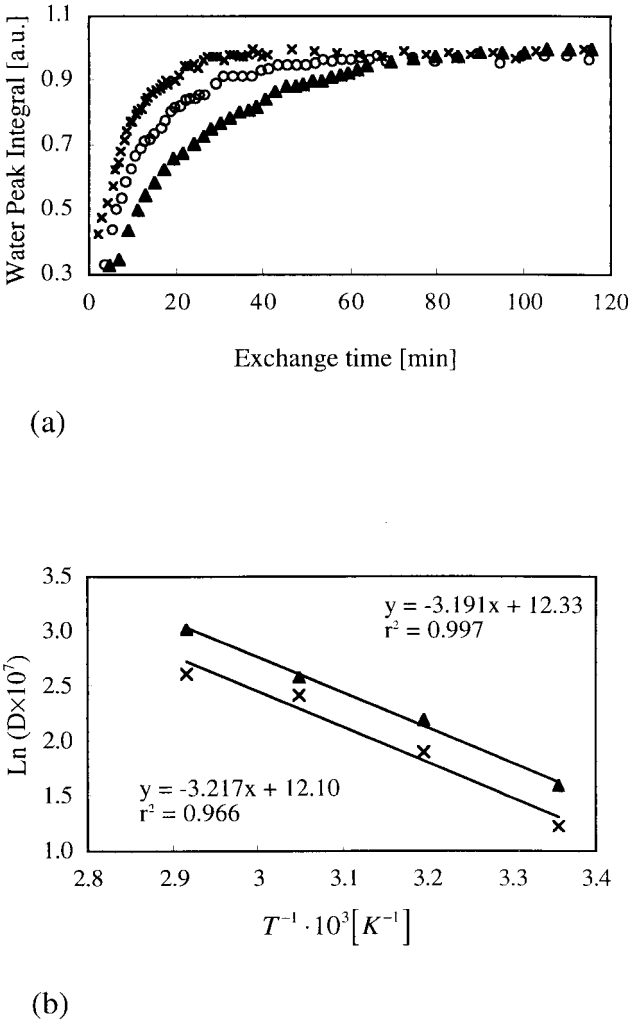

FIGURE 3 (*a*) Experimental exchange curves obtained at 25°C (▲), 40°C (○), and 55°C (×) showing the temperature dependence of the diffusion rate. (*b*) Arrhenius plots for two different cortical bone specimens. The slopes of the linear fits were used to compute the energy of activation for water diffusion.

Projection imaging of water diffusion and spatially resolved D_a

Fig. 4 shows the water profiles along the tibial cortex, obtained by projection imaging for specimen 2. As the exchange proceeds, H_2O is gradually replaced by (unobservable) D_2O, and the spatial distribution of the water changes. The profiles appear blurred due to the decay of the

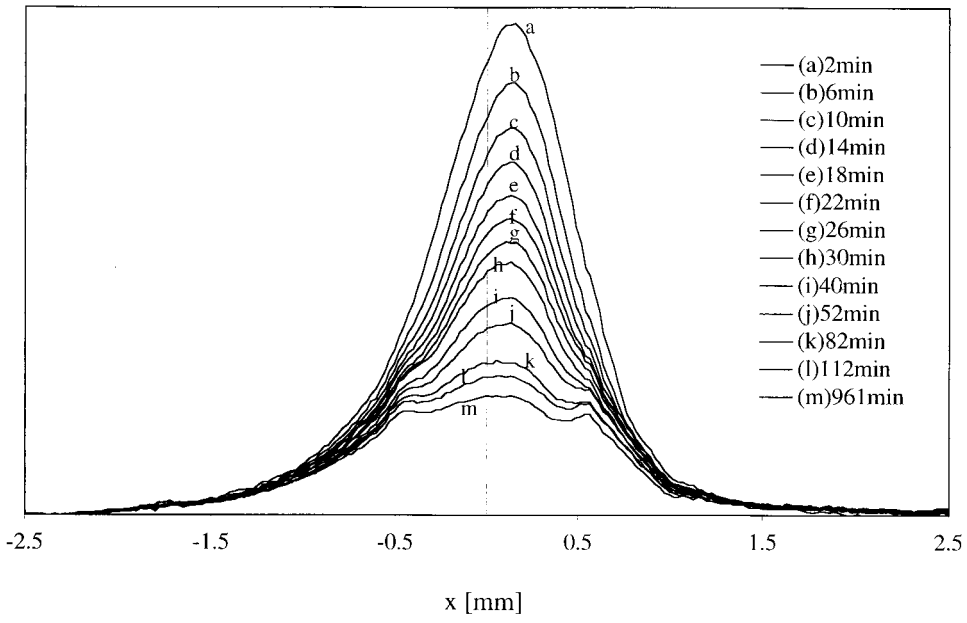

FIGURE 4 One-dimensional water profiles along the tibia cortex, acquired during proton-deuterium exchange. As the exchange progresses, the water content decreases, and its distribution changes. The last profile (*m*) was acquired 16 h after the beginning of the experiment. The profiles are blurred due to T_2* decay of the signal during the acquisition period. The width at half-maximum of the first profile (*a*) approximately corresponds to the thickness of the specimen.

signal during acquisition. The transverse relaxation time for the RF-reversible signal decay (T_2*), measured from the bone water spectrum (acquired in the absence of the imaging gradient), presents two major components (T_2* $\sim$ 125 μs and $\sim$ 13 μs). Fourier transformation of the time-domain signal that decays exponentially with time constant T_2*, results in a convolution of the actual water profile with a Lorentzian function (the point spread function) of line width $(\pi T_2^*)^{-1}$. This process degrades the resolution by blurring the one-dimensional spatial projections (Callaghan, 1991). The decay of the signal due to the short T_2* component is, in this case, responsible for the blurring observed in the projection images of Fig. 4. Despite the blurring of the profiles the full width at half maximum is in good agreement with the specimen's thickness.

The water proton signal from the solution is almost completely suppressed by saturation caused by the long T_1 of HDO (repetition time/$T_1 \approx 0.01$), as is evident in Fig. 4, which shows negligible signal levels in the region of the field of view outside the specimen projection signal for all profiles.

In Fig. 5 *a* the integrated signal intensity of the profiles has been plotted versus exchange time. Six hours after the start of the experiment, the signal intensity appears to have reached an equilibrium value, although there remains a significant fraction of nonexchanged H_2O in the specimen ($\sim$30% of the initial H_2O content). It is clear that this is not a true equilibrium because water continues to exchange even 20 h after immersion of the bone in deuterium oxide, albeit at a much lower rate. The exchange curve for times longer than 6 h is again linear with respect to the square root of the exchange time (Fig. 5 *b*). The slope of the regression line was used to estimate the diffusion coefficient for this process, assuming that the entire remaining water fraction exchanges at the same rate, and the result is approximately four orders of magnitude slower than the major water fraction diffusion coefficient ($D_a \approx 10^{-11}$ cm^2/s).

Fig. 6 displays the spatial distribution of D_a across the tibial cortex, resolved by the finite difference method, using the water profiles acquired experimentally for specimen 2 to compute the spatial and temporal derivatives of the water concentration. D_a increases from 1.24×10^{-7} cm^2/s at the center of the cortex to 3.67×10^{-7} cm^2/s at the endosteal surface.

DISCUSSION

Diffusion of substances in a porous composite material such as the calcified matrix of cortical bone takes place along the fluid-containing pores (Haversian canals, lacunae, canaliculi, intracellular pathways, and micropores permeating the bone matrix). Thus, the "apparent" diffusion coefficient is determined by the diffusion coefficient of the solute in the fluid that fills the pores, the interaction between solute molecules and matrix, the actual length of the diffusion path, and the matrix porosity. The apparent diffusion coefficient of water in cortical bone, measured in our experi-

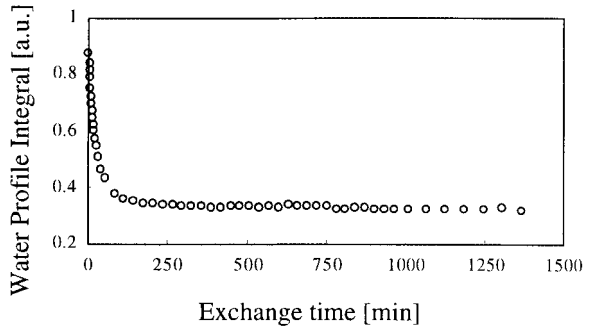

(a)

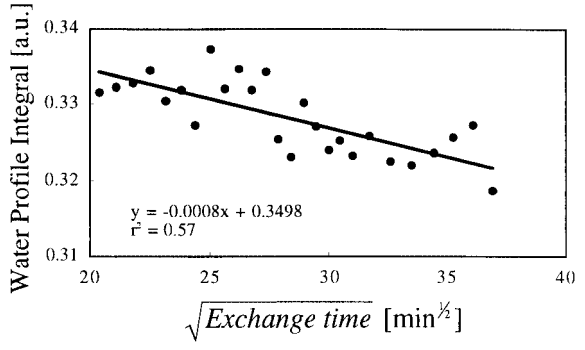

(b)

FIGURE 5 (*a*) The integral of the water profile (○) decreases as the D_2O/H_2O exchange progresses. (*b*) Water profile integral for exchange times greater than 6 h, plotted as a function of the square root of exchange time (●) and linear regression line. From the slope of the regression line the diffusion coefficient ($D_a \approx 10^{-11}$ cm^2/s) of the slow-exchange water component was estimated.

ments, is two orders of magnitude smaller than the self-diffusion coefficient of water ($D_{a\ bone} = (3.56 \pm 0.78) \times 10^{-7}$ cm^2/s, $D_{water} = 2.44 \times 10^{-5}$ cm^2/s at 25°C (Wang et al., 1953)). The ratio of these two values is an indication of the degree of porosity of the matrix and the actual distance traveled by the water molecules, assuming that the interaction between the water molecules and the channel walls does not significantly affect diffusion, which is a sensible assumption for molecules that are small, compared with the pore size (Maroudas, 1970). However, measurements of the energy of activation for water diffusion in cortical bone (E_a = 26.8 kJ/mol) result in higher activation energies than for diffusion in bulk water (E_a = 18.9 kJ/mol (Wang et al., 1953)), which implies that the bone matrix does present barriers to diffusion, by interaction between the water molecules and the matrix components, presumably in the form of hydrogen bonds.

Literature reports on quantitative diffusion measurements in bone are sparse. Neuman and Neuman (1981) performed

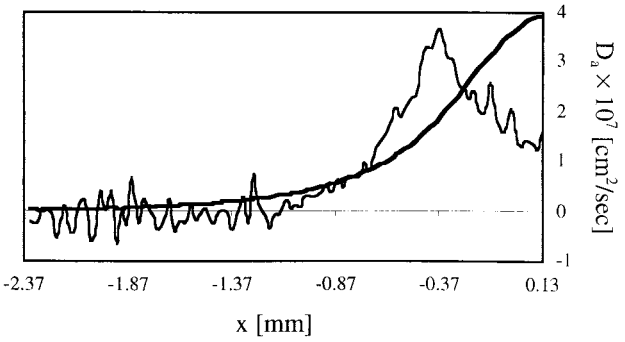

FIGURE 6 D_a profile along the tibia cortex, obtained from the water concentration profiles of Fig. 4, using a finite difference approximation to the diffusion equation. The D_a profile is shown for one-half of the tibia cortex with the center of the cortex being located at x = 0.13 mm. Superimposed on the D_a profile is the water profile at the beginning of the experiment (*bold line*).

studies of diffusion in rat calvaria, determining the rates of diffusion of small ions and neutral molecules. For comparison purposes, we have used the measured rates (reported in percentage clearance per hour normalized to 1 cm^2 cross-sectional area) to estimate the water diffusion coefficient. The result ($D = 1.8 \times 10^7$ cm^2/s) is in fair agreement with our own measurements.

Diffusion of water in cortical bone is two orders of magnitude faster than in enamel ($D_{enamel} = 3.5 \times 10^{-9}$ to 17×10^{-9} cm^2/s (Burke and Moreno, 1975)). The dissimilar behavior of the two calcified tissues can be explained by differences in their porosity. The enamel matrix, which is relatively homogenous compared with other calcified tissues, has a high mineral content, which at peak calcification, occupies ~85% of the matrix volume (93% of matrix wet weight), whereas the volume occupied by water is reduced to 10% (3.7% weight), which is consistent with the high density of fully mineralized enamel (2.79 mg/mm^3 (Deakins, 1942)). The matrix of cortical bone, on the other hand, contains more water, which for fully mineralized bone may exceed 20% by volume, thus reducing the matrix density to 2 mg/mm^3, (Robinson and Elliot, 1957). Diffusion of water in intertubular dentine is faster than in cortical bone ($D_{dentine} = (1.74 \pm 0.43) \times 10^{-6}$ cm^2/s (van der Graaf and ten Bosch, 1990)). Although the ranges of mineral fraction are similar in bone and dentine, the density of cortical bone is known to vary significantly with the type of bone and the anatomical location. In this work we have used dense cortical bone specimens, which probably explains the difference in diffusion rates.

In general, osteocytes are located within 100 to 150 μm of the Haversian canals (Martin and Burr, 1989), which constitute the bone vascular system and are the source of nutrient supply. Based on the value of D_a measured at 40°C (close to the physiological temperature) we estimate that it would take 1.24 min for a water molecule to travel 100 μm

in the cortical bone matrix. This result is in agreement with qualitative studies of diffusion using fluorescent tracers in tibial rat bone in vivo (Tate et al., 1998). Here, the authors observed that supply of small molecules to osteocytes by diffusive transport mechanisms via the lacunocanlicular system occurred within minutes after the tracers were introduced intravenously. Diffusive transport of water, in vivo, is presumably faster than it occurs under the conditions of our experiments, because the water content of the bone matrix under physiological conditions is higher, since some bone water is lost by evaporation after excision from the body and equilibration with the atmosphere (Smith and Walmsley, 1959).

The average water content of the bone specimens, measured using gravimetric methods (11.1 $\pm$ 0.4 weight %) is in the normal range for cortical bone (Robinson and Elliot, 1957). NMR-derived measurements of cortical bone water show that all or almost all the matrix water displaced by drying at 100°C is exchangeable. This observation agrees with reported studies of water exchange using deuterium oxide, in vivo, (Edelman et al., 1954), which found that 95% of the water contained in samples from the cortex of radius and femur dog bone (collected by vacuum distillation for 8 to 12 h) exchanges after 2 to 4 h. Drying at 100°C, however does not displace the water associated with the mineral phase (Robinson, 1960a).

The water profiles obtained by projection imaging, as the H_2O/D_2O exchange takes place, indicate that there is a significant H_2O fraction that still exchanges 6 h after the beginning of the experiment. The exchange rate for this process is four orders of magnitude slower than diffusion of the major water fraction. Presumably, this water is tightly bound to the organic matrix and the mineral phase and diffuses along the micropores that are embedded in the collagen and hydroxy-apatite matrix. On the average, the size of these micropores is an order of magnitude smaller than the size of canaliculi (Cooper et al., 1966; Holmes et al., 1964); the smaller pore size, together with stronger interaction between this water fraction and the bone matrix could explain the slower transport rate. The existence of tightly bound water in bone has been investigated previously using gravimetric methods (Robinson, 1960b) and in dielectric studies (Marino et al., 1967) where a critical hydration value of 37 to 49 mg H_2O/g bone was determined, below which water is assumed to be bound and above which it is free.

The spatially resolved diffusion profiles show that diffusion rates are higher close to the endosteal and periosteal surfaces and lower toward the center of the cortex, which presumably reflects differences in porosity across the cortex.

CONCLUSIONS

NMR imaging and spectroscopy based on monitoring the H_2O/D_2O exchange kinetics has proved to be uniquely suited for studying diffusion rates of water through the calcified matrix of compact bone, thus yielding detailed insight into the diffusional transport mechanisms across the bone matrix. It is concluded that transport of small molecules from the Haversian system to osteocytes takes on the order of minutes. The activation energy for the diffusion process indicates that interactions between the water molecules and the matrix pores present significant barriers to diffusion. The finite difference method used to resolve the D_a profile across the tibial cortex allowed observation of variations in transport properties on a local scale, which are probably related with changes in tissue microstructure and porosity. Finally, the data support the hypothesis of the existence of at least two different water fractions in the cortical bone matrix.

The authors are indebted to Dr. H. K. Song and Dr. J. Fernández-Seara for helpful discussion.

REFERENCES

Ayasaka, N., T. Kondo, T. Goto, M. A. Kido, E. Nagata, and T. Tanaka. 1992. Differences in the transport systems between cementocytes and osteocytes in rats using microperoxidase as a tracer. *Arch. Oral Biol.* 37:363–369.

Borthakur, A., R. Reddy, and F. W. Wehrli. 1998. NMR studies of exchangeable hydrogen in bone. *In* Proceedings of the International Society for Magnetic Resonance in Medicine, Sixth Annual Meeting, April 18–24, 1998, Sydney, Australia.

Burke, E. J., and E. C. Moreno. 1975. Diffusion fluxes of tritiated water across human enamel membranes. *Arch. Oral Biol.* 20:327–332.

Callaghan, P. T. 1991. T_2-limited resolution. *In* Principles of Nuclear Magnetic Resonance Microscopy. Oxford University Press Inc., New York. 189–201.

Cooper, R. R., J. W. Milgram, and R. A. Robinson. 1966. Morphology of the osteon: an electron microscopic study. *J. Bone Jt. Surg. Am.* 48: 1239–1271.

Crank, J. 1957. The Mathematics of Diffusion. Oxford University Press, London.

Deakins, M. 1942. Changes in the ash, water, and organic content of pig enamel during calcification. *J. Dent. Res.* 21:429–435.

Dillaman, R. M., R. D. Roer, and D. M. Gay. 1991. Fluid movement in bone: theoretical and empirical. *J. Biomech.* 24:163–177.

Edelman, I. S., A. H. James, H. Baden, and F. D. Moore. 1954. Electrolyte composition of bone and the penetration of radiosodium and deuterium oxide into dog and human bone. *J. Clin. Invest.* 33:122–131.

Holmes, J. M., D. H. Davies, W. J. Meath, and R. A. Beebe. 1964. Gas adsorption and surface structure of bone mineral. *Biochemistry.* 3:2019–2024.

Marino, A. A., R. O. Becker, and C. H. Bachman. 1967. Dielectric determination of bound water of bone. *Phys. Med. Biol.* 12:367–378.

Maroudas, A. 1970. Distribution and diffusion of solutes in articular cartilage. *Biophys. J.* 10:365–379.

Martin, R. B., and D. B. Burr. 1989. Structure, Function, and Adaptation of Compact Bone. Raven Press, New York.

Mueller, K. H., A. Trias, and R. D. Ray. 1966. Bone density and composition: age-related and pathological changes in water and mineral content. *J. Bone Jt. Surg. Am.* 48:140–148.

Neuman, W. F., and M. W. Neuman. 1958. Skeletal dynamics. *In* The Chemical Dynamics of Bone Mineral. University of Chicago Press, Chicago, IL. 101.

Neuman, W. F., and M. W. Neuman. 1981. Studies of diffusion in calvaria. *Calcif. Tissue Int.* 33:441–444.

Robinson, R. A. 1960a. Chemical analysis and electron microscopy of bone. *In* Bone as a Tissue. K. Rodahl, J. T. Nicholson, and E. M. Brown, editors. McGraw-Hill Book Company, New York. 186–250.

Robinson, R. A. 1960b. Crystal collagen water relationships in bone matrix. *Clin. Orthop.* 17:69–76.

Robinson, R. A., and S. R. Elliot. 1957. The water content of bone. *J. Bone Jt. Surg.* 39A:167–188.

Sasaki, T., A. Yamaguchi, S. Higashi, and S. Yoshiki. 1985. Uptake of horseradish peroxidase by bone cells during endochondral bone development. *Cell Tissue Res.* 239:547–553.

Smith, J. W., and R. Walmsley. 1959. Factors affecting the elasticity of bone. *J. Anat.* 93:504–523.

Stein, W. D. 1962. Diffusion and osmosis. *In* Comprehensive Biochemistry, Vol. 2. Elsevier, Amsterdan. 282–309.

Tate, M. L., and U. Knothe. 2000. An ex vivo model to study transport processes and fluid flow in loaded bone. *J. Biomech.* 33:247–254.

Tate, M. L., P. Niederer, and U. Knothe. 1998. In vivo tracer transport through the lacunocanalicular system of rat bone in an environment devoid of mechanical loading. *Bone.* 22:107–117.

Timmins, P. A., and J. C. Wall. 1977. Bone water. *Calcif. Tissue Res.* 23:1–5.

van der Graaf, E. R., and J. J. ten Bosch. 1990. The uptake of water by freeze-dried human dentine sections. *Arch. Oral Biol.* 35:731–739.

van der Graaf, E. R., and J. J. ten Bosch. 1991. Temperature dependence of water transport into the mineralized matrix of freeze-dried human dentine. *Arch. Oral Biol.* 36:177–182.

Wang, J. H., C. V. Robinson, and I. S. Edelman. 1953. Self-diffusion and structure of liquid water: III. Measurement of the self-diffusion of liquid water with ^{2}H, ^{3}H and ^{18}O as tracers. *J. Am. Chem. Soc.* 75:466–470.